



HHS Public Access

Author manuscript

Nat Commun. Author manuscript; available in PMC 2013 July 08.

Published in final edited form as:

Nat Commun. 2013 ; 4: 1338. doi:10.1038/ncomms2334.

Germinal centre protein HGAL promotes lymphoid hyperplasia and amyloidosis via BCR-mediated Syk activation

Isabel Romero-Camarero^{1,*}, Xiaoyu Jiang^{2,*}, Yasodha Natkunam³, Xiaoqing Lu², Carolina Vicente-Dueñas¹, Ines Gonzalez-Herrero¹, Teresa Flores¹, Juan Luis Garcia¹, George McNamara⁴, Christian Kunder³, Shuchun Zhao³, Victor Segura⁵, Lorena Fontan⁵, Jose A. Martínez-Climent⁵, Francisco Javier García-Criado⁶, Jason D. Theis⁷, Ahmet Dogan⁷, Elena Campos-Sánchez⁸, Michael R. Green⁹, Ash A. Alizadeh⁹, Cesar Cobaleda⁸, Isidro Sánchez-García^{1,Ψ}, and Izidore S. Lossos^{2,10,Ψ}

¹Experimental Therapeutics and Translational Oncology Program, Instituto de Biología Molecular y Celular del Cáncer, CSIC/Universidad de Salamanca and Institute of Biomedical Research of Salamanca (IBSAL), Salamanca, Spain

²Division of Hematology-Oncology, University of Miami, Sylvester Comprehensive Cancer Center, Miami, FL, USA

³Department of Pathology, Stanford University School of Medicine, Stanford, CA, USA

⁴Analytical Imaging Core Facility (AICF), University of Miami, Miami, FL, USA

⁵Division of Oncology, Center for Applied Medical Research (CIMA), University of Navarra, Pamplona, Spain

⁶Department of Surgery, University of Salamanca, Salamanca, Spain

⁷Department of Laboratory Medicine and Pathology, Mayo Clinic, Rochester, MN, USA

⁸Centro de Biología Molecular Severo Ochoa, CSIC/Universidad Autónoma, 28049 Madrid, Spain

⁹Divisions of Hematology and Oncology, Department of Medicine, Stanford University School of Medicine, Stanford, USA

¹⁰Department of Molecular and Cellular Pharmacology, University of Miami, Miami, FL, USA

Abstract

Users may view, print, copy, download and text and data- mine the content in such documents, for the purposes of academic research, subject always to the full Conditions of use: http://www.nature.com/authors/editorial_policies/license.html#terms

^ΨCorresponding authors: Izidore S Lossos M.D., Professor of Medicine, Sylvester Comprehensive Cancer Center, University of Miami, 1475 N.W. 12th Ave., (D8-4), Miami, Florida 33136, Phone: 305-243-4785, Fax: 305-243-4787, ILossos@med.miami.edu. Isidro Sanchez-Garcia (isg@usal.es); tel.: 34-923238403; fax: 34-923294813.

*Contributed equally

AUTHOR CONTRIBUTIONS

Isabel Romero-Camarero, Xiaoyu Jiang, Yasodha Natkunam- performed experiments and analyzed the data and wrote the paper; Xiaoqing Lu, Carolina Vicente-, Ines Gonzalez-Herrero, Teresa Flores, Juan Luis Garcia, George McNamara, Christian Kunder, Shuchun Zhao, Victor Segura, Lorena Fontan, Jose A. Martínez-Climent, Francisco Javier García-Criado, Jason D. Theis, Ahmet Dogan, Elena Campos-Sánchez, Michael R. Green, Ash A. Alizadeh, Cesar Cobaleda performed experiments and analysis data; Isidro Sánchez-García and Izidore S. Lossos - designed the study, analyzed the data, wrote the paper and contributed equally to this manuscript.

All the authors reviewed the manuscripts and agree with its content and do not have conflicts of interest relevant to this manuscript

The human germinal centre associated lymphoma (*HGAL*) gene is specifically expressed in germinal centre B-lymphocytes and germinal centre-derived B-cell lymphomas, but its function is largely unknown. Here we demonstrate that *HGAL* directly binds Syk in B-cells, increases its kinase activity upon B-cell receptor stimulation and leads to enhanced activation of Syk downstream effectors. To further investigate these findings *in vivo*, *HGAL* transgenic mice were generated. Starting from 12 months of age these mice developed polyclonal B-cell lymphoid hyperplasia, hypergammaglobulinemia and systemic reactive AA amyloidosis, leading to shortened survival. The lymphoid hyperplasia in the *HGAL* transgenic mice are likely attributable to enhanced B-cell receptor signalling as shown by increased Syk phosphorylation, *ex vivo* B-cell proliferation and increased RhoA activation. Overall, our study shows for the first time that the germinal centre protein *HGAL* regulates B-cell receptor signalling in B-lymphocytes which, without appropriate control, may lead to B-cell lymphoproliferation.

Keywords

HGAL; BCR signaling; Syk; lymphoid hyperplasia; amyloidosis

The *HGAL* gene is expressed in germinal center (GC) B-lymphocytes and GC-derived B-cell lymphomas^{1, 2}. In diffuse large B-cell lymphoma (DLBCL) and classic Hodgkin lymphoma patients, *HGAL* expression is associated with improved survival^{1, 3, 4}. The function of its murine homolog *M17* is unknown; knockout mice demonstrated reduced-size Peyer's patches but *M17* protein was dispensable for GC formation and function⁵. *In vitro* studies in human lymphocytes demonstrated that *HGAL* decreases cell motility by interacting with F-actin, myosin II and RhoA-specific guanine nucleotide exchange factors⁶⁻⁸. *HGAL* induced RhoA effects not only on cell migration but also on gene expression⁷. These findings suggest that *HGAL* may contribute to the control of GC lymphocyte motility but do not explain the biological relevance of GC specific *HGAL* expression.

The *HGAL* protein harbors a modified immunoreceptor tyrosine-based activation motif (ITAM) frequently used for B-cell receptor (BCR) signal transduction. BCR signaling is initiated upon antigen binding to membrane immunoglobulin (Ig), inducing receptor aggregation and Src kinase family-mediated tyrosine phosphorylation of ITAMs in signal transducing elements Ig- α and Ig- β ⁹. ITAM phosphorylation creates docking sites for Syk SH2 domains. Recruitment to the Ig- α/β facilitates Syk phosphorylation, leading to activation of signaling molecules that couple the BCR to multiple downstream signaling pathways. Consequently, Syk plays a key role in BCR signaling and its disruption leads to a block in B-cell development¹⁰⁻¹².

The presence of the ITAM, whose tyrosines can be phosphorylated by Lyn^{2, 6}, in the *HGAL* protein, raised a hypothesis that it might be involved in BCR signaling. We demonstrate that *in vitro* *HGAL* enhances BCR signaling by binding and increasing Syk activation. To further investigate these findings *in vivo*, *HGAL* transgenic mice were generated. Although young mice exhibited normal B-cell development, older *HGAL* transgenic animals progressively developed polyclonal lymphoid hyperplasia and reactive AA amyloidosis.

Overall our findings implicate HGAL in regulating BCR signalling, suggesting that it may play a role in humoral immune responses.

RESULTS

HGAL enhances intracellular BCR signaling

We analyzed HGAL's effect on the BCR pathway in response to surface Ig stimulation (Figure 1a). In unstimulated lymphoma cells there was no evidence for Syk, Btk and PLC γ 2 phosphorylation (not shown). Following BCR stimulation, Syk, Btk and PLC γ 2 phosphorylation was markedly reduced in lymphoma cell lines upon knockdown of endogenous HGAL by different siRNAs (Figure 1a and Supplementary Figure S1a), while Ig- α/β phosphorylation was not affected (not shown). Concordantly, ectopic HGAL expression in lymphoma cells and human peripheral B-lymphocytes lacking endogenous HGAL protein resulted in increased Syk phosphorylation (Figures 1a–b).

In activated B-lymphocytes, Btk, PLC γ 2 and BLNK constitute the calcium (Ca $^{2+}$) initiation complex, inducing release of intracellular Ca $^{2+}$ and activating protein kinase C (PKC), nuclear factor of activated T cells (NFAT), nuclear factor κ B (NF κ B) and mitogen-activated protein kinase (MAPK) signaling^{9, 13}. Consequently, we examined the effects of HGAL gain and loss of function on the ability of lymphoma cells to mobilize Ca $^{2+}$ in response to BCR stimulation. Following Ig stimulation, HGAL expression in HBL1 cells led to increased Ca $^{2+}$ mobilization (not shown), while HGAL knockdown in Raji, VAL and BJAB cells markedly reduced Ca $^{2+}$ mobilization (Figure 1c and Supplementary Figure S1b). HGAL knockdown in lymphoma cells transfected with constructs containing either NFAT or NF κ B responsive luciferase reporter genes resulted in significantly decreased reporter activity (Figure 1d and Supplementary Figure S1c). HGAL knockdown in lymphoma cells also led to decreased ERK1/2 and p38 phosphorylation, while JNK phosphorylation was unaffected (Figure 1e and Supplementary Figure S1d), consistent with previous reports¹⁴. Overall, these findings show that HGAL affects BCR signaling downstream of the Ig- α/β proteins.

HGAL interacts with Syk and enhances its kinase activity

Syk plays a major role in coupling BCR activation to downstream effectors. Since Syk selectively binds to phosphorylated ITAM¹⁰, we examined for a potential interaction between HGAL and Syk. Endogenous Syk was detected in immunoprecipitates of endogenous HGAL from unstimulated Raji and VAL lymphoma cells (Figure 2a and not shown). BCR stimulation increased HGAL and Syk co-immunoprecipitation (co-IP) (Figure 2a). HGAL protein did not co-immunoprecipitate with Lyn, Ig- α/β p, Btk, BLNK and PLC γ 2 in unstimulated and BCR-stimulated lymphoma cells (not shown). Nanoscope microscopy of unstimulated Raji cells confirmed HGAL and Syk colocalization in the cell membrane (Figure 2b); BCR stimulation further increased HGAL/Syk colocalization, in concordance with the co-IP findings. A GST pull down assay using purified GST-Syk, GST-Grb2 or GST and TRX-HGAL proteins demonstrated a direct, specific interaction. GST-Syk pulled-down TRX-HGAL; however, non-phosphorylated HGAL did not bind to GST-Grb2 and GST proteins (Figure 2c).

To determine whether the Syk tandem SH2 domains mediate interaction with HGAL protein, we transiently co-transfected wild type HGAL with truncated Syk encoding the tandem SH2 domains (amino acids 1–261) into Raji and 293T cells and repeated the co-IP experiments. Truncated Syk protein was detected in the HGAL immunoprecipitates (Figure 2d and Supplementary Figure S2a), indicating that HGAL protein interacts with the Syk tandem SH2 domains.

To determine the HGAL interacting domain, HGAL mutants encoding N-terminal 79 (1–79) or 118 (1–118) aa segments and tyrosine mutants (Y128F, Y148F and Y106AY107A) (Supplementary Figure S2b) were co-transfected with the wild type Syk into VAL and 293T cells and co-IP experiments were repeated (Figure 2e and Supplementary Figure S2c). Individual mutations of HGAL tyrosines and HGAL truncations did not affect Syk binding, suggesting that the first 79aa of HGAL were sufficient to mediate Syk binding.

We next examined whether the HGAL protein stimulates Syk kinase activity. Syk protein was immunoprecipitated from BCR stimulated or unstimulated Raji cells and used in the kinase assay, either alone or with purified HGAL protein (Figure 2f). No Syk kinase activity was observed in unstimulated cells, even in the presence of HGAL protein. In stimulated cells, addition of HGAL protein markedly increased Syk kinase activity, suggesting that HGAL binding to Syk enhances its kinase activity in BCR-stimulated cells, underlying the observed increased Syk autophosphorylation and activation of its downstream effectors

HGAL gain-of-function mouse model

To examine HGAL effects on the immune system and BCR signaling *in vivo*, a Sca1-HGAL plasmid encoding human *HGAL* cDNA under the control of the mouse *Ly-6E.1* promoter¹⁵ (Figure 3a–b) was used to generate a transgenic mouse model in which HGAL is expressed in Sca1⁺ hematopoietic stem (HSC)/progenitor cells and Sca1⁺ fraction of mature B cells of C57BL/6 x CBA mice¹⁶. A similar approach recapitulated gene functions and generated animal models highly similar to human diseases^{17–19}. Two independent Sca1-HGAL founder lines (102A and 102B) exhibited normal embryonic and post-natal development and were used to characterize the transgenic mice phenotype.

A Southern blot comparison of the endogenous M17 and transgenic human HGAL hybridization signals indicated transgene copy numbers ranging from 2 to 4 (Figure 3b). Flow cytometry studies revealed that only a fraction of B220 splenocytes expressed Sca1. Similar fractions of B220 splenocytes in young Sca1-HGAL (4–8 week-old) and control mice expressed Sca1 (Supplementary Figure S3a). While there was a tendency for a smaller Sca1 expressing fraction of B220 splenocytes in older (starting at 12 months of age) Sca1-HGAL mice compared to control animals, it was not statistically significant (Supplementary Figure S3a). Immunofluorescence studies using antibody to the V5 tag, fused to *HGAL* in the plasmid used to generate the transgenic animal, detected ectopically expressed human HGAL in both BM and spleen cells (Figure 3c), with no difference in expression between young and old animals. HGAL expression was not detected in either mature myeloid, monocyte and T-cell lineages or in the wild type controls. Overall, HGAL protein expression levels were similar to levels observed in the human U2OS cell line transfected with the same HGAL plasmid used to generate the transgenic construct (Supplementary

Figure S3b). There was no difference in the endogenous M17 mRNA expression between Sca1-HGAL and littermate splenocytes (Supplementary Figure S3c).

Lymphoid hyperplasia and amyloidosis in Sca1-HGAL mice

A total of 75 transgenic animals were analyzed. Compared to age-matched controls, 8 week-old Sca1-HGAL animals did not show any visible changes within the major hematopoietic compartments (BM, spleen, thymus, peripheral blood and lymph nodes (LN)) by flow cytometry and histological examinations (Figure 4a, Supplementary Figure S4).

Immunization with sheep red blood cells led to GC formation in both transgenic and wild-type mice. Flow cytometry analyses did not reveal statistically significant differences in the number of splenic B220⁺PNA⁺Fas⁺GL7⁺ GC B cells between the Sca1-HGAL and control animals (Supplementary Figure S5a). Immunohistochemistry also did not reveal differences in the size and number of GCs in the spleens of immunized Sca1-HGAL and control mice (Supplementary Figure S5b), indicating that young Sca1-HGAL mice respond normally to T-cell dependent antigen stimulation.

Starting at 12 months of age, the Sca1-HGAL mice demonstrated increased-sized Peyer's patches compared to control animals (Figure 3d) and expressed HGAL protein at levels similar to ones observed in human Payer's patches. These animals also exhibited non-statistically significant decrease in number of BM immature and pro- and pre-B-cells at the expense of recirculating B-cells (B220⁺IgD^{hi}) (Figure 4a–b). All the Sca1-HGAL mice became ill, showing decreased spontaneous movements in the cage, increased respiratory rates, piloerection and shivering, and died between 12 to 22 months, exhibiting statistically significant shorter overall survival (Figure 5a).

Macroscopic analysis of these animals revealed massive splenomegaly (Figure 5b). The overall microscopic architecture of the spleen was preserved; however, the splenic sinusoids were dilated and distorted by large quantities of proteinaceous deposits, which were also present surrounding small and medium-caliber splenic blood vessels (Figure 5c). These deposits were found adjacent to expanded white pulp areas showing lymphoid hyperplasia with preserved periarteriolar lymphoid sheaths. Immunohistochemistry using B220 and PAX5 antibodies highlighted a significant proportion of the expanded white pulp representing B-cells, whereas CD3 highlighted a slightly smaller proportion of T-cells. B220 staining was weak compared to that of PAX5, although both stains showed an equivalent distribution of B-cells. Staining for IRF4 highlighted T-cell areas in addition to a few scattered plasmacytoid cells. PNABio showed no significant staining within the white pulp, suggesting that white pulp expansions represented lymphoid hyperplasia without GC formation (Figure 5c). Control animals showed a similar distribution of B and T-cells within the white pulp, although without lymphoid hyperplasia (Supplementary Figure S6a). In both Sca1-HGAL and control animals, CD38 (not shown) and CD138 showed weak expression in the B-cells without the intense expression typically seen in plasma cells (Figure 5c and Supplementary Figure S6a). Flow cytometry also did not demonstrate differences in the number and percentage of B220^{lo}CD138⁺ splenic cells between young and old Sca1-HGAL and control mice (Supplementary Figure S6b). In contrast, flow cytometry analysis detected IgM⁺ B-cells in peripheral blood and BM (Figure 5d-e), confirming that the observed

splenic lymphoid hyperplasia was due to follicular (FO) B-cells (Figure 5f). The percentage of Sca1⁺Lin⁻ cells in BM did not increase in Sca1-HGAL mice compared to normal littermates (data not shown). Analysis of the B-1 lymphocyte population in the older animals revealed a significant decrease in B-1 cell number and percentage in the spleen and a significant increase in the LN of the Sca1-HGAL mice compared to normal littermates (Supplementary Figure S4). There was no difference in the number and percentage of B-1 and B-1a cells in the BM and peritoneum between the Sca1-HGAL and control animals.

Congo red and trichrome stains of the spleens for amyloid showed distinctive positive staining of the proteinaceous deposits; Congo red showed the characteristic muted orange color on light microscopy and exhibited apple-green birefringence under polarized light. Similarly, the trichrome stain showed a grayish-blue color, consistent with amyloid deposition and in contrast to the bright turquoise blue that is typically demonstrated by collagen (Figure 5c). Tissue sections from multiple organs including the kidney, liver, lung and small intestine showed similar massive amyloid deposition (Supplementary Figure S7a–b). Sections of the kidney, liver and lung showed preservation of the normal architecture with modest mixed lymphoid infiltrates that were absent in control animals. Massive amyloid deposition was observed in all renal glomeruli as well as the interstitium. Amyloid deposition was also seen surrounding small and medium caliber blood vessels in the kidneys, lung and liver, but not the heart. Electron microscopy of spleen specimens confirmed the presence of amyloid deposits (Supplementary Figure S7c–d). Liquid chromatography tandem mass spectrometry (LC MS/MS) analysis of the kidney and spleen specimens showed that the most abundant pathogenic protein in the amyloid deposits was serum amyloid associated protein-2 (SAA2), consistent with AA amyloidosis (Figure 6). Analysis of SAA2 peptide sequences revealed the absence of 33aa of the C-terminus, suggesting these residues were cleaved during the amyloidogenesis, similar to what has been described in human AA amyloidosis²⁰. Like in human amyloidosis, constituents of many human amyloid types (apolipoprotein E, apolipoprotein A-IV, serum amyloid P-component and apolipoprotein A-I) were also detected in the amyloid deposits in the Sca1-HGAL mice.

To examine whether the observed lymphoid hyperplasia were of clonal origin, DNA extracted from the splenic B-lymphocytes from Sca1-HGAL mice were subjected to Southern blot using the 3' J_H4 probe. No immunoglobulin heavy chain (*IgH*) gene rearrangements were detected (Supplementary Figure S8a). Polymerase chain reactions followed by direct sequencing or cloning and sequencing of multiple molecular clones also failed to detect predominant monoclonal products (Supplementary Figure S8b), further indicating that the observed lymphoid hyperplasia were of polyclonal origin. Cytogenetic and FISH studies of the splenic B-lymphocytes from lymphoid hyperplasia demonstrated normal karyotypes without evidence for *Bcl2-IgH* translocation (not shown).

Sca1-HGAL transgenic mice display hypergammaglobulinemia

The presence of polyclonal FO B-cell lymphoid hyperplasia in the Sca1-HGAL transgenic mice pointed to possible immune stimulation, potentially leading to hypergammaglobulinemia. The non-immunized Sca1-HGAL mice produced antibodies of

all isotypes and IgG titers tended to be higher than in the wild-type controls, reaching statistical difference for IgG1 isotype (Figure 7a).

Enhanced BCR signaling in lymphoid hyperplasia splenocytes

The observed lymphoid hyperplasia in the Sca1-HGAL mice might be attributed to increased B-cell proliferation due to enhanced BCR signalling or to promotion of B-cell survival. To differentiate between these mechanisms, we examined *ex vivo* B-cell proliferation in response to BCR stimulation (Figure 7b). There was no difference in cell proliferation rates between control and young Sca1-HGAL mouse groups at all analyzed IgM concentrations. In contrast, B-cells from Sca1-HGAL mice with lymphoid hyperplasia demonstrated increased proliferation to 0.5 and 2 $\mu\text{g/ml}$ anti-IgM antibody concentrations compared to both wild-type controls and young transgenic mice. However, B-cell proliferation was similar in all the three types of animals at saturating 8 $\mu\text{g/ml}$ anti-IgM antibody concentrations. Splenic B-cell surface Ig expression was similar in all the three types of analyzed animals (not shown). These findings suggest that B-lymphocytes from Sca1-HGAL mice with lymphoid hyperplasia show enhanced sensitivity to surface Ig stimulation. Concordantly, increased Ca^{2+} mobilization (Figure 7c) and Syk phosphorylation (Figure 7d) were observed in the BCR-stimulated B-cells from Sca1-HGAL mice with lymphoid hyperplasia compared to control animals. In contrast, isolated B220+ splenocytes from Sca1-HGAL transgenic and control mice supplemented only with 5% fetal calf serum exhibited a similar *in vitro* overtime death rate (Supplementary Figure S9), suggesting that HGAL does not promote B-cell survival in the Sca1-HGAL mice.

RhoA activation in Sca1-HGAL transgenic mice

Our previous *in vitro* studies demonstrated that HGAL induces RhoA activation in human B-cells⁷. Consequently, we examined the levels of GTP-bound RhoA in B-cell splenocytes isolated from Sca1-HGAL transgenic mice with and without lymphoid hyperplasia. RhoA-GTP levels were significantly higher in Sca1-HGAL B-cells from spleens with versus without lymphoid hyperplasia ($p=0.006$, analyzed by 2-tailed Student *t* test) (Figure 7e), corroborating the observed activation of this pathway in human B-cells.

Transcriptome changes in Sca1-HGAL transgenic mice

To comprehensively assess the global effect of HGAL on lymphocyte functions and the observed lymphoproliferation, we performed gene expression profiling using isolated CD22+B220+ splenocytes from adult Sca1-HGAL mice with hyperplastic follicles and wild-type littermates (4 samples each).

In supervised analyses using Significance Analysis of Microarrays (SAM)²¹ at a 10% FDR, we identified 981 genes with significantly increased expression in B-splenocytes from adult Sca1-HGAL mice with lymphoid hyperplasia compared to controls (Supplementary Data 1). Figure 8a depicts 107 of these genes (Supplementary Data 2), focusing on those with at least 3-fold change between the specimens from Sca1-HGAL transgenic and control mice. In concordance with HGAL's role in regulating lymphocyte motility, gene expression profiles in the Sca1-HGAL mice with lymphoid hyperplasia apparently reflect 'Cell Movement' ($p=5.46e-9$, IPA) and 'Migration of Cells' ($p=0.0001$, IPA) as evidenced by significant

overlap with the corresponding pathways using the Ingenuity Pathway Analysis knowledgebase. Sca1-HGAL B-splenocytes also exhibited decreased mRNA expression of regulator of G-protein signaling 13 and 18 (RGS13 and RGS18), whose down-regulation may enhance the signaling activity of G-proteins potentially enhancing RhoA activation.

We also observed significant induction of BCR pathway components in the Sca1-HGAL mice (Figure 8a-b), including immunoglobulin heavy chain genes (Ighg1, Igh-2 [IgA], Ighg2b, Ighg2c), corroborating our observation of serum hypergammaglobulinemia (Figure 7a). Within these lymphoid hyperplasias we also observed significant induction of CD80 (Figure 8b), which co-stimulates T-lymphocytes, a finding which we confirmed at the protein level (Figure 8c), demonstrating CD80 expression in a fraction of B-lymphocytes. No significant differences in expression levels of mRNAs for CD86 (B7-2), CD69, CD5, or MHC-II antigens were detected.

To evaluate the relative representation of normal differentiation states within splenocytes from Sca1-HGAL mice with hyperplastic follicles compared to B-cells from wild-type littermates, we utilized gene set enrichment analysis (GSEA) of transcriptional profiling data. Classification signatures from normal murine stages of B-cell differentiation were obtained from Green et al.²² to assess expression bias in Sca1-HGAL compared to control B-cells. Gene expression signature corresponding to both the normal FO/Marginal Zone (FO/MZ) and the Plasma cell B-cell differentiation states were significantly enriched in Sca1-HGAL B-cells (Figure 8d-e). Conversely, signatures corresponding to the remaining differentiation states were significantly enriched in control B-cells, suggesting a relative over-representation of B-cells at the FO/MZ and plasma cell differentiation states in Sca1-HGAL mice with hyperplastic follicles. To further validate the role of HGAL in these B-cell differentiation states, we performed a reciprocal analysis of Sca1-HGAL signatures in transcriptional profiling data from normal murine B-cells²². Genes found to be highly expressed in Sca1-HGAL B-cells compared to control B-cells (Figure 8a) were tested for enrichment in normal FO/MZ and plasma B-cells and compared to B-cells of other differentiation states. This revealed a significant enrichment of HGAL-induced genes in normal FO/MZ B-cells, but not in normal plasma cells, compared to other differentiation states (Supplementary Figure S10a-c). The lack of significant enrichment in normal plasma cells is likely the result of down-regulation of a subset of HGAL-induced genes within this differentiation state. Together, these results suggest that Sca1-HGAL B-cells possess transcriptional signatures indicative of an over-representation of FO/MZ B-cells and plasma cells. However, immunohistochemistry and flow cytometry studies did not show an increase in plasma cells in the lymphoid hyperplasia observed in the Sca1-HGAL mice, suggesting that the B220+ cells may be poised toward plasma cell differentiation; however, induced transcriptional changes characteristic to plasma cells were insufficient to lead to plasma cell differentiation. Indeed, the observed transcriptional signatures lacked expression of *PRDMI* and *XBPI*, genes necessary for plasma cell genesis. Furthermore, normal murine FO/MZ B-cells had significantly enriched expression of HGAL-induced genes, suggesting that HGAL may play a role in normal FO/MZ B-cell biology.

We also compared the transcriptional responses evoked by HGAL in B-cell lymphoid hyperplasia of Sca1-HGAL mice to those induced in other B-cell tumors at various stages of

the B-cell lineage, with a focus on those arrested at the GC and beyond^{23, 24}. Notably, genes induced in the lymphoid hyperplasia in the Sca1-HGAL mice significantly overlapped those up-regulated in murine GC derived lymphomas driven by Bcl6²⁴ ($p=2.48e-4$ by hypergeometric test) (Supplementary Figure S10d) and were also enriched for those uniformly repressed within plasma cell tumors driven by Myc/Bcl-xL²³ ($p=1.8e-12$ by hypergeometric test) (Supplementary Figure S10e), suggesting a distinct regulatory program in these hyperplasia leading to immunoglobulin secretion.

DISCUSSION

The outcome of BCR stimulation is diverse and is determined by the maturation state of the cell, the nature and quantity of the antigen, signals from co-receptors and the magnitude and duration of BCR signaling. An “on-off” mode of BCR signal transduction would not allow for diverse cellular responses. Fine-tuning the magnitude and duration of BCR signaling and preferential activation of specific downstream signaling components by adaptor proteins selectively expressed during B-cell development is of paramount importance for B cell functional plasticity^{25, 26}. We demonstrate that the GC-specific adaptor HGAL regulates BCR signaling by direct binding and activation of Syk. While HGAL is not necessary for GC formation⁵, HGAL transgenic animals exhibited increased-size Peyer’s patches, a finding corroborating the reduced-size Peyer’s patches in the M17 knockout mice⁵. This observation suggests a specific function of HGAL in Peyer’s patches. Furthermore, it is possible that the increased-size HGAL expressing Peyer’s patches may contribute to systemic lymphoid hyperplasia and subsequent development of AA amyloidosis, which was never observed in the absence of lymphoid hyperplasia. HGAL-mediated enhancement of BCR signaling may be important for efficient and timely completion of the GC reaction and selective activation of signaling pathways (e.g. ERK and p38 but not JNK). Based on the presented mouse model, HGAL expression predisposes to lymphoid hyperplasia, polyclonal hypergammaglobulinemia and enhanced proliferation in response to BCR stimulation, culminating in systemic AA amyloidosis. B-lymphocytes in HGAL transgenic mice showed enhanced activation of Syk and RhoA signaling, suggesting this model recapitulates the biological effects of HGAL protein in human B-cells. The observed polyclonal lymphoid hyperplasia was characterized by an accumulation of FO lymphocytes in the absence of GC lymphocytes and terminally differentiated plasma cells. The FO B-cells in the lymphoid hyperplasia exhibited transcriptional signatures characteristic to FO/MZ B-cells and plasma cells and were accompanied by polyclonal hypergammaglobulinemia in the absence of mature plasma cells, suggesting a block in terminal plasma cell differentiation whose nature is currently unknown. Studies examining HGAL’s effects on transcriptional signatures in human B-cells are ongoing. In addition, whether the observed phenotype was due to expression of HGAL in the transgenic lines starting from progenitor and not specifically in the GC cells will need to be addressed.

B cell activation in the Sca1-HGAL mice led to reactive systemic AA amyloidosis not observed in the control animals. The molecular features and anatomical location of the observed amyloid deposits precisely recapitulated human AA amyloidosis complicating chronic inflammatory diseases (e.g. rheumatoid arthritis). In these diseases reactive follicular hyperplasia and lymphadenopathy are commonly observed²⁷ and frequently

precede development of systemic amyloidosis. Heretofore, temporary AA amyloid deposits were induced in mice by exogenous agents (e.g. casein, lipopolysaccharide), that would resolve without continued stimulation. Progressive and permanent AA amyloid deposits were observed in IL-6 and SAF-1 transgenic mice starting from 3–14 months of age^{28, 29}. In these models IL-6 and SAF-1 directly stimulated SAA production, bypassing the preceding chronic inflammatory state observed in human disease. Conversely, HGAL mice develop AA amyloid deposits in a similar timeframe and show systemic lymphoid hyperplasia and hypergammaglobulinemia preceding amyloidosis onset, therefore authentically recapitulating human amyloidosis associated with chronic inflammatory disorders. These mice may thus serve as an excellent model for this disease.

The polyclonal lymphoid hyperplasia observed in the Sca1-HGAL mice were similar to the lymphoid hyperplasia detected in the BCL2 transgenic mice models, which also displayed polyclonal hypergammaglobulinemia. However, the mechanisms underlying these phenomena were different (increased cell proliferation and decreased apoptosis, respectively)³⁰. Additional differences between these models are also noticeable. BCL2 transgenic mice develop lymphoid hyperplasia earlier than Sca1-HGAL mice, display autoimmune complex glomerulonephritis and a proportion of these animals develop lymphomas that were not detected in the Sca1-HGAL mice^{30–33}. In contrast, infiltration of normal organs by B-lymphocytes and amyloidosis was observed only in the Sca1-HGAL mice.

HGAL is expressed in the GC-derived B-cell lymphomas, but whether it has a role in lymphomagenesis is unknown. The Sca1-HGAL mice developed lymphoid hyperplasia, but not lymphomas. However, it is possible that HGAL may facilitate the transformation process. Gene expression arrays demonstrated significant overlap between genes upregulated in the lymphoid hyperplasia of the Sca1-HGAL mice and lymphomas driven by Bcl6/ λ Myc²⁴. It is possible that the BCR-mediated proliferation detected in the Sca1-HGAL mice may cooperate with the antiapoptotic effects induced by BCL2 or differentiation arrest induced by BCL6 during the transformation process. Previous studies demonstrated similar cooperation between BCR and Myc in the genesis of B-cell lymphomas³⁴. Use of the Sca1-HGAL mouse model to generate bitransgenic mice will help to elucidate the potential role of HGAL in lymphomagenesis.

METHODS

Mice and cell culture

Human non-Hodgkin lymphoma (NHL) cell lines Raji, VAL, BJAB and HBL-1 were grown as previously reported³⁵. Human B-lymphocytes were isolated from healthy donor blood using EasySep Human B cell enrichment kit (StemCell Technologies Inc, Vancouver, BC, Canada).

A Sca1-HGAL plasmid in which *HGAL* cDNA is under the control of the mouse Ly-6E.1 promoter was generated as follows: the fragment containing the human *HGAL-V5* cDNA, was inserted into the ClaI site of the pLy6 vector¹⁵, resulting in Sca1-HGAL vector. The transgene fragment (Figure 3A) was excised from the vector by restriction digestion with

NotI, purified for injection ($2 \text{ ng } \mu\text{l}^{-1}$) and injected into CBA \times C57BL/6J fertilized eggs. Transgenic mice were identified by Southern analysis of tail snip DNA after EcoRI digestion. *HGAL* cDNA was used as a probe for detection of the transgene. The transgene copy number was determined by Southern blot analysis using copy standards prepared by mixing non-transgenic tail DNA with a known amount of transgene DNA as described in Camper et al³⁶.

A total of 47 and 28 animals derived from founder lines 102A and 102B, respectively, housed in pathogen free conditions were used for the analyses. There were no differences between the founder lines. All animal experiments were performed in accordance with the guidelines of the Committees on Animal Research at University of Salamanca and University of Miami, and the National research Council.

For cell sorter separation, B220 and CD22 lineage markers were used to purify cells from the spleen of both Sca1-HGAL or control wild-type mice by fluorescence-activated cell sorting (FACS) (FACSVANTAGE; Becton Dickinson). Purity of the sorted cells was over 98%, as determined by FACS reanalysis. Alternatively, mouse B-lymphocytes were isolated from mice spleen using EasySep mouse B-cell enrichment kit (StemCell Technologies Inc).

For analysis of B1 and B2 lymphocyte populations, single-cell suspensions were obtained from the spleens, lymph nodes, bone marrow and peritoneal cavities of individual Sca1-HGAL and control mice. To obtain peritoneal cells, 6ml of ice cold PBS 1% FCS were injected into the peritoneal cavity using a 25g needle attached to a syringe. After injection, the peritoneum was gently massaged and cells were collected using a 5ml syringe. Cells were washed with PBS 1% FCS and incubated for at least 5 min with CD16/CD32 Fc Block (clone 2.4G2) to minimize background staining. A total of 2×10^6 cells were stained for 30 min on ice with IgD-FITC (clone 11-26c.2a), CD5-PE (clone 53-7.3), Mac1-PerCP-Cy5.5 (clone M1/70), and IgM-APC (II/41) to identify the B2 and B1 cell subsets. All the antibodies were purchased from the BD Pharmingen. At least 1×10^5 cells were acquired using a BD C6 Accuri (BD Biosciences) and analyzed by the Flowjo software (Tree Star Inc.)

Antibodies, plasmids and chemicals, as well as procedures for cell transfection, western blotting, immunoprecipitation, RhoA activity, GST pull down and luciferase reporter assays are described in the Supplementary Methods.

Flow cytometry and immunofluorescence microscopy

Nucleated cells were obtained from total bone marrow (flushing from the long bones), peripheral blood, thymus, lymph nodes and spleen. Contaminating red blood cells were lysed with RCLB lysis buffer and the remaining cells were then washed in PBS with 1% FCS. After staining, all cells were washed once in PBS with 1% FCS containing 2 mg/mL propidium iodide (PI) to allow dead cells to be excluded from both analyses and sorting procedures. The samples and the data were analyzed in a FACSCalibur using CellQuest (Becton Dickinson) or FlowJo (TreeStar) software. Specific fluorescence of FITC, PE, PI and APC excited at 488 nm (0.4 W) and 633 nm (30 mW), respectively, as well as known

forward and orthogonal light scattering properties of mouse cells were used to establish gates. For each analysis a total of at least 50,000 viable (PI⁻) cells were assessed.

FACS definition of B-cell developmental stages was performed according to Kwon et al.³⁷ with minor modifications: BM pro-B cells (CD19⁺c-Kit⁺), BM pre-B cells (B220⁺CD25⁺IgM⁻), BM immature B-cells (B220⁺IgM^{hi}IgD⁻), BM recirculating B-cells (B220⁺IgD^{hi}), peripheral transitional B-cells (B220⁺IgM^{hi}IgD^{hi}), peripheral mature-B cells (B220⁺IgM^{lo}IgD^{hi}), marginal zone (MZ) B-cells (B220⁺CD21^{hi}CD23^{lo}), follicular (FO) B-cells (B220⁺CD21^{int}CD23^{hi}).

The subcellular localization of HGAL and Syk was assessed by stimulated emission depletion (STED) fluorescence nanoscope images³⁸, as described in detail in the Supplementary Methods together with the methodology for the immunohistochemistry and analysis of amyloid fibril protein.

Gene expression analysis

Using flow cytometry, CD22⁺B220⁺ splenocytes from adult Sca1-HGAL mice with hyperplastic follicles and wild-type littermates (4 samples each) were sorted to ~98% purity, and profiled the corresponding gene expression patterns using Affymetrix GeneChip Mouse Gene 1.0 ST Arrays. Raw array microarray data files were submitted to GEO and are available under the accession number GSE35400. For probeset summarization, microarray CEL data files were subjected to a custom Chip Definition File (MoGene10stv1_Mm_ENTREZG_13.0.0) with a mapping of probes to Entrez Gene Identifiers as previously described³⁹. Gene level data were normalized using Robust Multichip Average (RMA) within the BioConductor environment⁴⁰. Significance Analysis of Microarrays (SAM)²¹ at a 10% False Discovery Rate was used to identify the probe sets with significant differential expression between experimental conditions. We used DAVID⁴¹, Ingenuity Pathway Analysis tools (IPA 9/2011 Release), and the Molecular Signatures Database (MSigDB, v3.0),⁴² to assess whether differentially expressed genes show functional enrichment.

For assessment of differentiation state, normal murine B-cell differentiation state signatures corresponding to Pro-B/Pre-B, Transitional, Follicular/Marginal Zone, Germinal center, plasmablast and plasma cell stages of differentiation were used as previously defined²². Over-representation of differentiation states within Sca1-HGAL compared to control B-cells was inferred by assessing comparative enrichment of normal differentiation state signatures using Gene Set Enrichment Analysis (GSEA)⁴². GSEA was performed using a weighted enrichment statistic, signal-to-noise ratio ranking metric, and corrected for multiple hypothesis testing (MHT) using 10,000 permutations to provide an MHT-corrected false discovery rate (FDR) q-value. Reciprocal analysis was performed in order to validate positive enrichments within Sca1-HGAL B-cells. Therein, publicly available gene expression data of normal murine B-cell differentiation states (GSE26408) was used to probe for enrichment of HGAL-induced genes within the Follicular/Marginal Zone and Plasma cell differentiation states compared to all other differentiation states (1-versus-all analysis) using GSEA.

Statistical analysis

To test the differences in responses between cells, we used the two way Anova test for ex vivo B-cell proliferation assay and 2-tailed Student *t* test for remaining experiments. Mice survival curves were estimated using the product-limit method of Kaplan-Meier and were compared using the log-rank test. *P* values less than .05 were considered statistically significant.

Supplementary Material

Refer to Web version on PubMed Central for supplementary material.

Acknowledgments

Grant support: *I.S.L. is supported by National Institutes of Health (NIH) grants NIH CA109335 and NIH CA122105, and the Dwoskin Family Foundations. YN is supported by NIH P01 CA34233. Research in ISG group was partially supported by FEDER and by MICINN (SAF2009-08803 and SAF2012-32810 to ISG), by Junta de Castilla y León (REF. CSI007A11-2 and Proyecto Biomedicina 2009–2010), by MEC OncoBIO Consolider-Ingenio 2010 (Ref. CSD2007-0017), by Sandra Ibarra Foundation, by Group of Excellence Grant (GR15) from Junta de Castilla y Leon, and the ARIMMORA project (FP7-ENV-2011, European Union Seventh Framework Program) and by Proyecto en Red de Investigación en Celulas Madre Tumorales en Cancer de Mama, supported by Obra Social Kutxa y Conserjería de Sanidad de la Junta de Castilla y Leon.*

References

1. Lossos IS, Alizadeh AA, Rajapaksa R, Tibshirani R, Levy R. HGAL is a novel interleukin-4-inducible gene that strongly predicts survival in diffuse large B-cell lymphoma. *Blood*. 2003; 101:433–440. [PubMed: 12509382]
2. Pan Z, et al. Studies of a germinal centre B-cell expressed gene, GCET2, suggest its role as a membrane associated adapter protein. *Br J Haematol*. 2007; 137:578–590. [PubMed: 17489982]
3. Natkunam Y, et al. Expression of the human germinal center-associated lymphoma (HGAL) protein, a new marker of germinal center B-cell derivation. *Blood*. 2005; 105:3979–3986. [PubMed: 15677569]
4. Natkunam Y, et al. Expression of the human germinal center-associated lymphoma (HGAL) protein identifies a subset of classic Hodgkin lymphoma of germinal center derivation and improved survival. *Blood*. 2007; 109:298–305. [PubMed: 16954503]
5. Schenten D, Egert A, Pasparakis M, Rajewsky K. M17, a gene specific for germinal center (GC) B cells and a prognostic marker for GC B-cell lymphomas, is dispensable for the GC reaction in mice. *Blood*. 2006; 107:4849–4856. [PubMed: 16493007]
6. Lu X, et al. HGAL, a lymphoma prognostic biomarker, interacts with the cytoskeleton and mediates the effects of IL-6 on cell migration. *Blood*. 2007; 110:4268–4277. [PubMed: 17823310]
7. Jiang X, et al. HGAL, a germinal center specific protein, decreases lymphoma cell motility by modulation of the RhoA signaling pathway. *Blood*. 2010; 116:5217–5227. [PubMed: 20844236]
8. Lu X, et al. Germinal center-specific protein human germinal center associated lymphoma directly interacts with both myosin and actin and increases the binding of myosin to actin. *FEBS J*. 2011; 278:1922–1931. [PubMed: 21447067]
9. Niiro H, Clark EA. Regulation of B-cell fate by antigen-receptor signals. *Nat Rev Immunol*. 2002; 2:945–956. [PubMed: 12461567]
10. Sada K, Takano T, Yanagi S, Yamamura H. Structure and function of Syk protein-tyrosine kinase. *J Biochem*. 2001; 130:177–186. [PubMed: 11481033]
11. Turner M, et al. Perinatal lethality and blocked B-cell development in mice lacking the tyrosine kinase Syk. *Nature*. 1995; 378:298–302. [PubMed: 7477352]
12. Cheng AM, et al. Syk tyrosine kinase required for mouse viability and B-cell development. *Nature*. 1995; 378:303–306. [PubMed: 7477353]

13. Koretzky GA, Abtahian F, Silverman MA. SLP76 and SLP65: complex regulation of signalling in lymphocytes and beyond. *Nat Rev Immunol.* 2006; 6:67–78. [PubMed: 16493428]
14. Jiang A, Craxton A, Kurosaki T, Clark EA. Different protein tyrosine kinases are required for B cell antigen receptor-mediated activation of extracellular signal-regulated kinase, c-Jun NH2-terminal kinase 1, and p38 mitogen-activated protein kinase. *J Exp Med.* 1998; 188:1297–1306. [PubMed: 9763609]
15. Miles C, Sanchez MJ, Sinclair A, Dzierzak E. Expression of the Ly-6E.1 (Sca-1) transgene in adult hematopoietic stem cells and the developing mouse embryo. *Development.* 1997; 124:537–547. [PubMed: 9053329]
16. Fossati V, Kumar R, Snoeck HW. Progenitor cell origin plays a role in fate choices of mature B cells. *J Immunol.* 2010; 184:1251–1260. [PubMed: 20038638]
17. Perez-Caro M, et al. Cancer induction by restriction of oncogene expression to the stem cell compartment. *The EMBO journal.* 2009; 28:8–20. [PubMed: 19037256]
18. Vicente-Dueñas C, et al. Expression of MALT1 Oncogene in Hematopoietic Stem/Progenitor Cells Recapitulates the Pathogenesis of Human Lymphoma in Mice. *Proc Natl Acad Sci U S A.* 2012; 109:10534–10539. [PubMed: 22689981]
19. Vicente-Duenas C, et al. A novel molecular mechanism involved in multiple myeloma development revealed by targeting MafB to haematopoietic progenitors. *The EMBO journal.* 2012; 31:3704–3717. [PubMed: 22903061]
20. van der Hilst JC. Recent insights into the pathogenesis of type AA amyloidosis. *The Scientific World Journal.* 2011; 11:641–650. [PubMed: 21403980]
21. Tusher VG, Tibshirani R, Chu G. Significance analysis of microarrays applied to the ionizing radiation response. *Proc Natl Acad Sci U S A.* 2001; 98:5116–5121. [PubMed: 11309499]
22. Green MR, et al. Signatures of murine B-cell development implicate Yy1 as a regulator of the germinal center-specific program. *Proc Natl Acad Sci U S A.* 2011; 108:2873–2878. [PubMed: 21282644]
23. Boylan KLM, et al. A Transgenic Mouse Model of Plasma Cell Malignancy Shows Phenotypic, Cytogenetic, and Gene Expression Heterogeneity Similar to Human Multiple Myeloma. *Cancer Research.* 2007; 67:4069–4078. [PubMed: 17483317]
24. Pasqualucci L, et al. AID is required for germinal center-derived lymphomagenesis. *Nat Genet.* 2008; 40:108–112. [PubMed: 18066064]
25. Marshall AJ, et al. A novel B lymphocyte-associated adaptor protein, Bam32, regulates antigen receptor signaling downstream of phosphatidylinositol 3-kinase. *J Exp Med.* 2000; 191:1319–1332. [PubMed: 10770799]
26. Shlapatska LM, et al. CD150 association with either the SH2-containing inositol phosphatase or the SH2-containing protein tyrosine phosphatase is regulated by the adaptor protein SH2D1A. *J Immunol.* 2001; 166:5480–5487. [PubMed: 11313386]
27. Kojima M, Motoori T, Nakamura S. Benign, atypical and malignant lymphoproliferative disorders in rheumatoid arthritis patients. *Biomedicine & pharmacotherapy = Biomedecine & pharmacotherapie.* 2006; 60:663–672. [PubMed: 17064872]
28. Solomon A, et al. Transgenic mouse model of AA amyloidosis. *Am J Pathol.* 1999; 154:1267–1272. [PubMed: 10233864]
29. Ray A, Shakya A, Kumar D, Benson MD, Ray BK. Inflammation-responsive transcription factor SAF-1 activity is linked to the development of amyloid A amyloidosis. *J Immunol.* 2006; 177:2601–2609. [PubMed: 16888022]
30. McDonnell TJ, et al. bcl-2-immunoglobulin transgenic mice demonstrate extended B cell survival and follicular lymphoproliferation. *Cell.* 1989; 57:79–88. [PubMed: 2649247]
31. Xiang H, et al. The immunoglobulin heavy chain gene 3' enhancers induce Bcl2 deregulation and lymphomagenesis in murine B cells. *Leukemia.* 2011; 25:1484–1493. [PubMed: 21606958]
32. Egle A, Harris AW, Bath ML, O'Reilly L, Cory S. VavP-Bcl2 transgenic mice develop follicular lymphoma preceded by germinal center hyperplasia. *Blood.* 2004; 103:2276–2283. [PubMed: 14630790]
33. Strasser A, et al. Enforced BCL2 expression in B-lymphoid cells prolongs antibody responses and elicits autoimmune disease. *Proc Natl Acad Sci U S A.* 1991; 88:8661–8665. [PubMed: 1924327]

34. Refaeli Y, et al. The B cell antigen receptor and overexpression of MYC can cooperate in the genesis of B cell lymphomas. *PLoS Biol.* 2008; 6:e152. [PubMed: 18578569]
35. Sarosiek KA, et al. Novel IL-21 signaling pathway up-regulates c-Myc and induces apoptosis of diffuse large B-cell lymphomas. *Blood.* 2010; 115:570–580. [PubMed: 19965678]
36. Camper SA. Research Applications of Transgenic Mice. *Biotechniques.* 1987; 5:638–650.
37. Kwon K, et al. Instructive role of the transcription factor E2A in early B lymphopoiesis and germinal center B cell development. *Immunity.* 2008; 28:751–762. [PubMed: 18538592]
38. Willig KI, Harke B, Medda R, Hell SW. STED microscopy with continuous wave beams. *Nat Methods.* 2007; 4:915–918. [PubMed: 17952088]
39. Dai M, et al. Evolving gene/transcript definitions significantly alter the interpretation of GeneChip data. *Nucleic acids research.* 2005; 33:e175. [PubMed: 16284200]
40. Irizarry RA, et al. Summaries of Affymetrix GeneChip probe level data. *Nucleic acids research.* 2003; 31:e15. [PubMed: 12582260]
41. Dennis G Jr, et al. DAVID: database for annotation, visualization, and integrated discovery. *Genome Biol.* 2003; 4:P3. [PubMed: 12734009]
42. Subramanian A, et al. Gene set enrichment analysis: A knowledge-based approach for interpreting genome-wide expression profiles. *Proceedings of the National Academy of Sciences of the United States of America.* 2005; 102:15545–15550. [PubMed: 16199517]

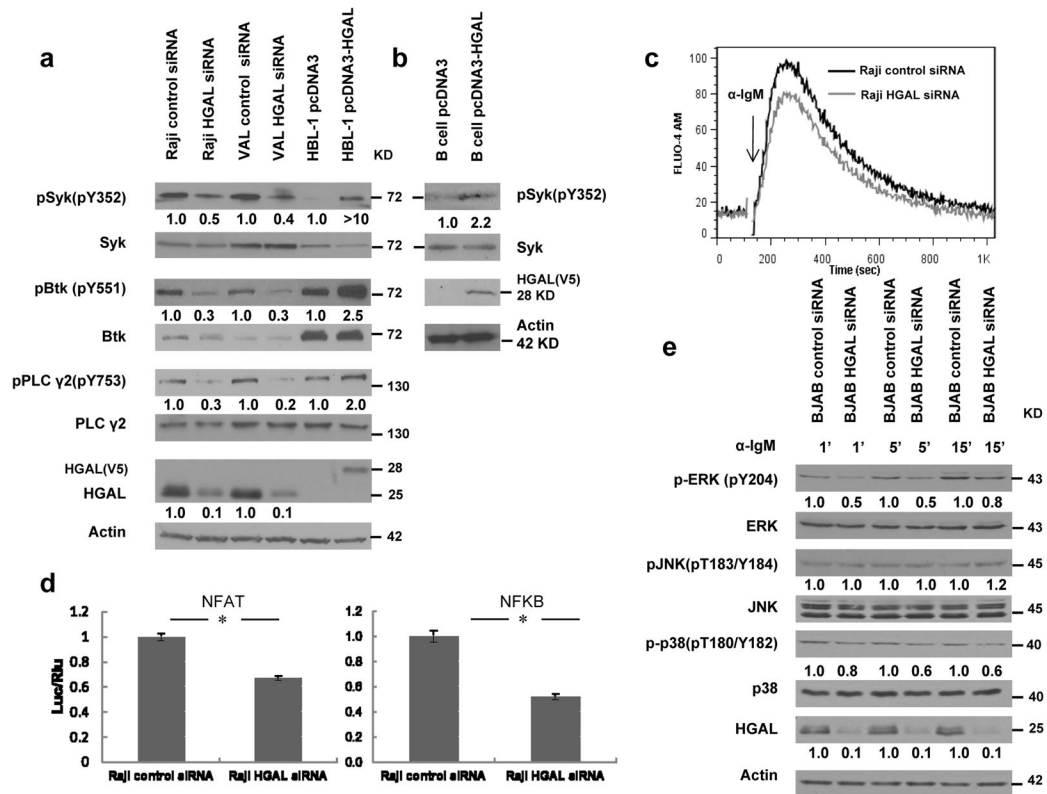


Figure 1. HGAL enhances intracellular BCR signaling

Raji and VAL lymphoma cells were transfected with siRNA for HGAL or scrambled control siRNA and HBL-1 cells (a) and normal peripheral blood B-lymphocytes (b) transfected with pcDNA3.1-HGAL or pcDNA3.1-mock plasmids for 48 hours. After 1 minute stimulation with goat F(ab')₂ anti-human IgM, western blot of BCR receptor effectors was performed. HGAL expression and equal loading were analyzed by immunoblotting with HGAL and actin antibodies. (c) Kinetic of calcium mobilization in Raji cells transfected with siRNA for HGAL or scrambled control siRNA. Arrow indicated the time point of goat F(ab')₂ anti-human IgM stimulation. (d) Raji lymphoma cells were transfected with firefly luciferase reporter plasmid pNFκB-Luc or pNFAT-Luc and Renilla luciferase plasmid pRL-TK and with either siRNA for HGAL or scrambled control siRNA. 48 hours after transfection the cells were stimulated for 10 min with goat F(ab')₂ anti-human IgM and luciferase activities were detected with the Dual Luciferase assay kit. Numbers refer to luciferase activities representing 3 independent experiments, each performed in triplicate. * indicate statistically significant difference (NFκB p=0.0001 and NFAT p=0.001 by 2-tailed Student *t* test). Data are presented as mean ± SD of the mean. (e) BJAB lymphoma cells were transfected with siRNA for HGAL or scrambled control siRNA for 48 hours. After stimulation with goat F(ab')₂ anti-human IgM, cell lysates were used for western blot of MAPK/ERK pathway effectors at indicated time points. HGAL knock down or expression and equal loading were confirmed by immunoblotting with HGAL and actin antibodies. Normalized densitometry measurements are shown below the corresponding blots. Results in (a–e) are representative of 3 independent experiments.

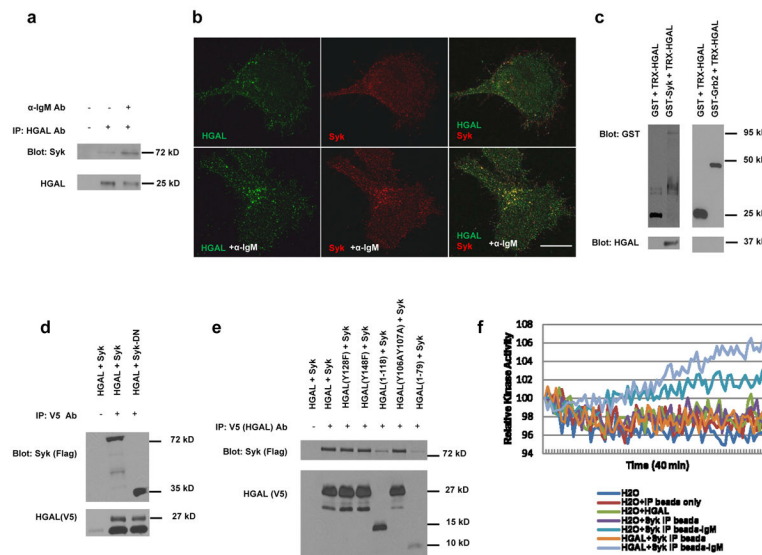


Figure 2. HGAL interacts with Syk and stimulates its kinase activity

(a) Cell lysates extracted from unstimulated and goat F(ab')₂ anti-human IgM stimulated (1 min) Raji lymphoma cells were subjected to immunoprecipitation with anti-HGAL or control antibodies followed by anti-HGAL and anti-Syk western blot, respectively. (b) Unstimulated or stimulated Raji cells (as described in (a)) were stained with HGAL (green) and Syk (red) antibodies. Scale bar 10 μm. (c) Purified GST-Syk, GST-Grb2 or GST proteins were incubated with TRX-HGAL protein for 12 h. The co-precipitated HGAL and Syk or Grb2 proteins were detected by western blot with anti-GST and anti-HGAL antibodies. (d) Raji cells were transfected with wild type Syk or its dominant negative Syk-DN mutant plasmids and HGAL tagged with V5 plasmid. Cells lysates were immunoprecipitated with anti-V5 or control antibodies and analyzed by western blot with anti-Syk and anti-HGAL antibodies. (e) VAL cells were transfected with Syk plasmid and V5-tagged plasmids encoding wild type HGAL or its C-terminal truncated mutants HGAL (1–79) or HGAL(1–118), or tyrosine mutants HGAL(Y106AY107A), HGAL(Y128F) or HGAL(Y148F). Cells lysates were immunoprecipitated with anti-V5 or control antibodies and analyzed by western blot with anti-Syk and anti-HGAL antibodies. (f) Syk was immunoprecipitated from unstimulated or stimulated Raji cells as described in (a) and used in Syk kinase activity measurement, either alone or with purified HGAL protein. Immunoprecipitates with control antibody and beads only, purified HGAL alone and water were used as negative controls. Results in (a–f) are representative of 2 (c) or 3 independent experiments.

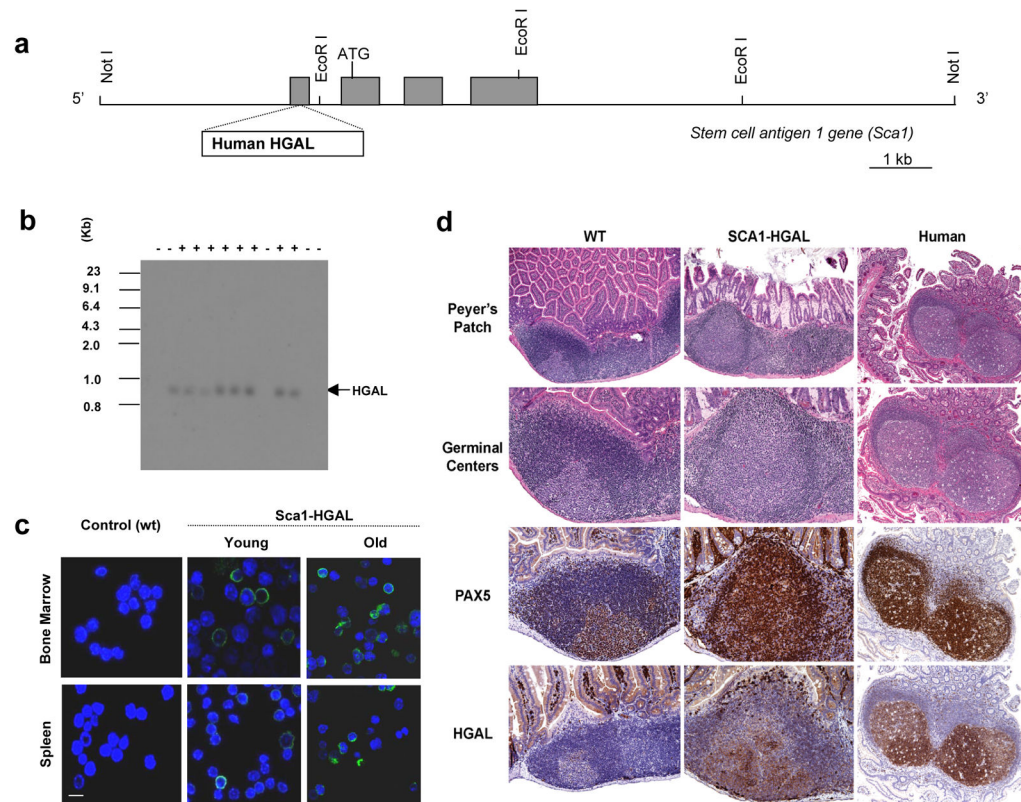


Figure 3. HGAL gain-of-function mouse model

(a) Schematic representation of the genomic structure of the mouse *Sca1* locus and the Sca-1-HGAL transgenic vector used to generate transgenic animals. (b) Identification of the transgenic mice (n=75) by Southern analysis of tail snip DNA after EcoRI digestion. Sca1-HGAL is indicated. (c) HGAL expression in Sca1-HGAL mice. Bone marrow and spleen cells of control (n=3) and Sca1-HGAL mice (n=3) were stained with anti-V5 antibody (green) and DAPI (blue) and examined under a microscope. Data are representative of three independent experiments. Scale bar 10 μ m (d) Representative sections of ileum show increased-sized Peyer's patches and prominent germinal centers stained with PAX5 and HGAL in Sca1-HGAL compared to control mice. All mouse images were photographed at comparable magnifications: x100, Peyer's patches panels; x300, remaining panels. Human Peyer's patches are shown for comparison (x40, Peyer's patches panel, x80, remaining panels).

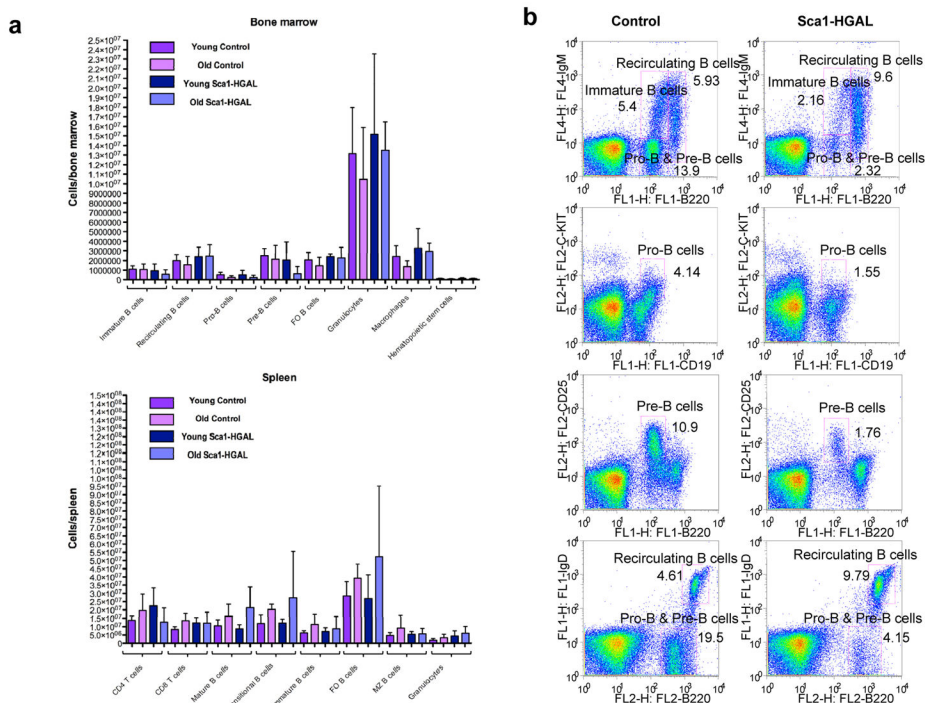


Figure 4. Analysis of the bone marrow and spleen cell lineages in the Sca1-HGAL mice
 Cells from the bone marrow (BM) and spleen of young (8 weeks) and old (more than 7 month old) age-matched Sca1-HGAL mice and wild type controls (n=11 in each group) were analyzed by flow cytometry. (a) Total cell number of the indicated cell subpopulations in the BM and spleens of the young and old Sca1-HGAL and control mice. Data are presented as mean ± SD of the mean. (b) Representative FACS plots of 12 month old Sca1-HGAL mice are displayed. FACS definition of B-cell developmental stages was performed according to Kwon³⁷.

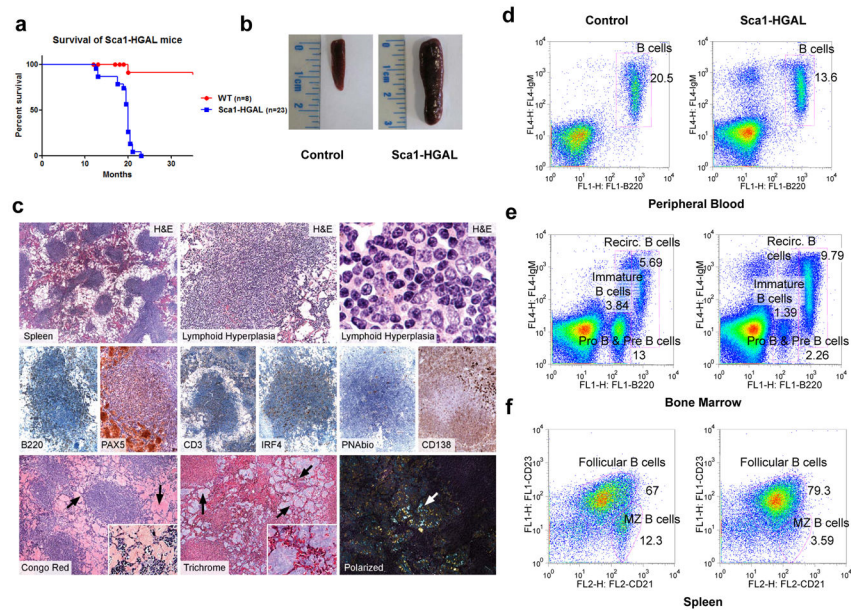


Figure 5. B-cell lymphoid hyperplasia in Sca1-HGAL mice

(a) Kaplan-Meier overall survival plots of Sca1-HGAL mice. The total numbers of mice analyzed in each group were 8 wild-type control mice and 23 Sca1-HGAL transgenic mice. Differential survival in Sca1-HGAL and control mice was analyzed using the Log-rank test ($p=0.0000003$). (b) Sca1-HGAL mice develop massive splenomegaly. Data is representative of pathologic analysis of 36 Sca1-HGAL transgenic mice. (c) Representative sections of spleen of Sca1-HGAL mice show overall preservation of microscopic architecture; however, the splenic sinusoids were dilated and distorted by large quantities of proteinaceous deposits (spleen hematoxylin and eosin (H&E) panel original magnification I x40; lymphoid hyperplasia panels original magnifications x100 and x400). These deposits were found adjacent to lymphoid hyperplasia which was highlighted by B220 (weak positive staining) and PAX5 representing B-cells, and a smaller proportion of CD3-positive T-cells. Staining for IRF4 highlighted T-cell areas in addition to a few scattered plasmacytoid cells while PNAbio (a GC marker) showed no significant staining to indicate GC formation. CD138 showed weak expression in the B-cells without the intense expression typically seen in plasma cells (B220, PAX5, CD3, IRF4, PNAbio and CD138 panels, x200 original magnification). Congo red (orange staining) and trichrome (grayish-blue) stains highlight amyloid deposits, which under polarized light, showed the characteristic apple-green birefringence (x400 original magnification). (d–f) Representative FACS plots of peripheral blood (d), bone marrow (e) and spleen (f) lymphocytes from Sca1-HGAL mice with lymphoid hyperplasia ($n=15$) and control littermates ($n=15$).

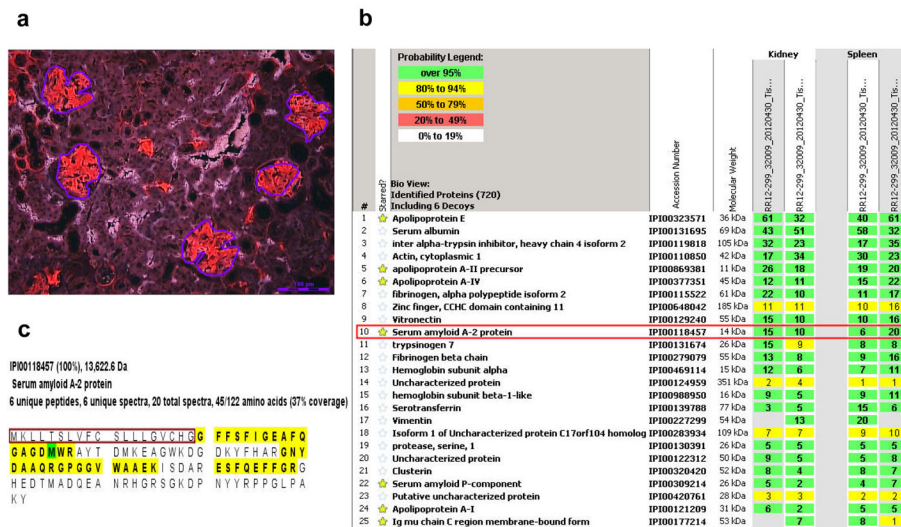


Figure 6. Analysis of amyloid fibrils
 (a) Congo red stained kidney specimen viewed under fluorescent light source with bright red areas representing amyloid deposits. Purple colored lines - areas microdissected for mass spectrometry-based proteomic analysis. (b) Results of mass spectrometry based proteomic analysis of amyloid plaques from the kidney and spleen specimens in 2 independent microdissections. The identified proteins are listed according to their relative abundance, with top 25 from a total of 720 proteins shown. The columns show the protein name, the UniProt identifier (protein accession number in the UniProt database, <http://www.uniprot.org/>), the molecular weight of the protein, two microdissections of the kidney specimen and two microdissections of the spleen specimen. The numbers indicate number of total peptide spectra identified for each protein. The amyloid associated proteins are identified by yellow stars. The peptides representing the serum amyloid A-2 protein (red box) are the primary cause of amyloid deposits in the Sca1-HGAL mouse model. (c) SAA2 protein coverage in the Sca1-HGAL mouse amyloidosis model. The amino acid (aa) sequence of the SAA2_MOUSE is provided. The yellow highlights indicate the parts of the protein that were identified by the LC MS/MS. The first 19aa represent the N-terminus signal peptide of the SAA2_MOUSE (red box) cleaved before the mature SAA2_MOUSE is secreted into the circulation, and thus is not expected to be part of the amyloid deposits. The peptides missing in the middle of the protein are unlikely to be detected by LC MS/MS due to abundance of numerous trypsin cutting sites.

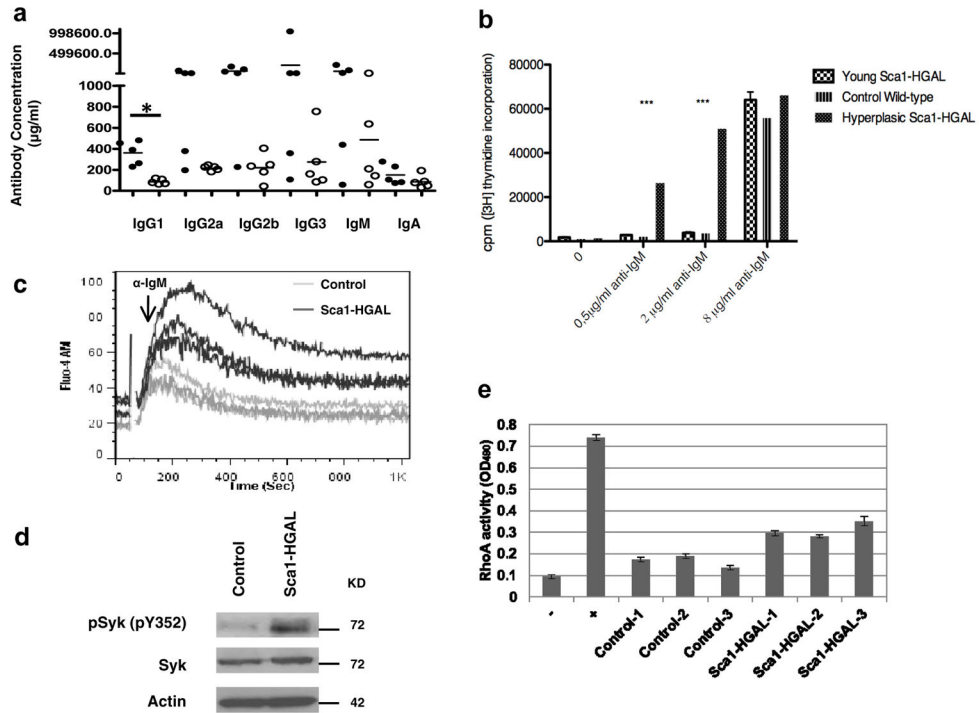


Figure 7. Hypergammaglobulinemia and enhanced BCR and RhoA signaling in the Sca1-HGAL mice

(a) Immunoglobulin isotype titers in the serum of 14 month old unimmunized control (open circles) and Sca1-HGAL (black circles) mice analyzed by ELISA. n=5 per group. * indicates $p=0.0007$ by 2-tailed Student *t* test. (b) *Ex vivo* B-cell proliferation in response to surface Ig stimulation. Purified splenic B cells from wild type mice, young Sca1-HGAL transgenic mice without lymphoid hyperplasia and Sca1-HGAL transgenic mice with lymphoid hyperplasia (3 animals in each group) were stimulated with the indicated concentrations of an anti-IgM antibody and cell proliferation assessed by [³H]thymidine incorporation in triplicates. Shown is mean \pm SEM. *** indicates statistically significant difference: for 0.5 $\mu\text{g/ml}$ anti-IgM $p=0.000004$ and for 2 $\mu\text{g/ml}$ anti-IgM $p=0.0000007$ by two way analysis of variance test. (c) Kinetic of calcium mobilization measured by flow cytometry in purified spleen B-lymphocytes from 3 Sca1-HGAL transgenic mice with lymphoid hyperplasia (black) and 3 wild type control mice (gray). Arrow indicates the time point of stimulation with goat F(ab')₂ anti-mouse IgM. (d) Purified spleen B-lymphocytes from Sca1-HGAL transgenic or control mice stimulated with goat F(ab')₂ anti-mouse IgM for 1 min were used for western blot with pSyk (pY352) and total Syk antibodies. Equal loading was confirmed by immunoblotting with actin antibodies. (e) Purified spleen B-cells from Sca1-HGAL transgenic or wild type control mice stimulated with 1 $\mu\text{g/ml}$ lysophosphatidic acid (LPA) for 45 seconds were used for RhoA activity measurement in triplicates; lysis buffer served as negative control and RhoA protein as a positive control. Shown is mean \pm SD. Results in (d) and (e) are representative of 3 independent experiments.

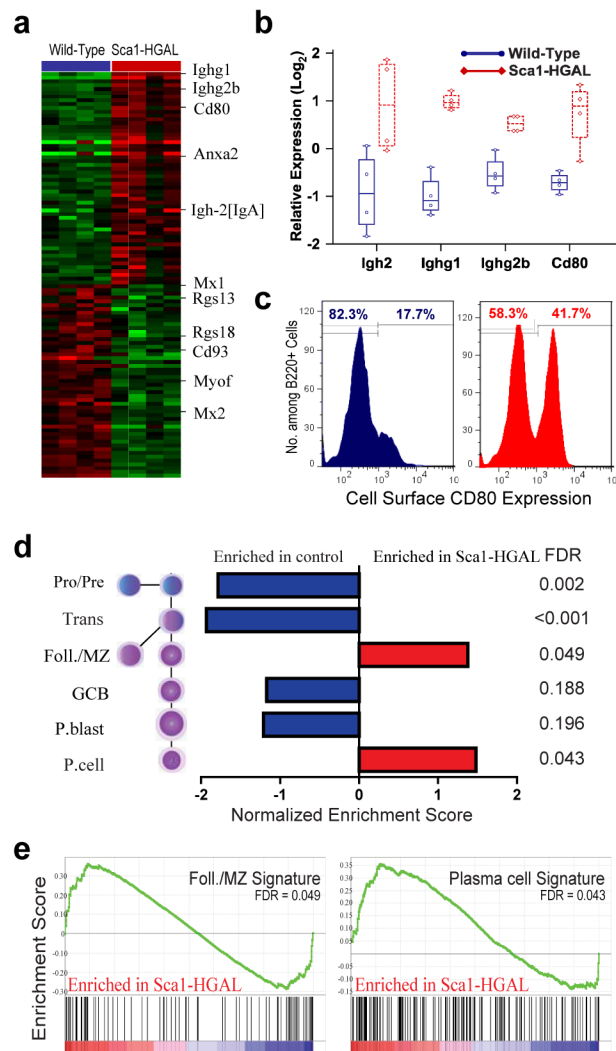


Figure 8. Transcriptional signatures evoked *in vivo* within B-cell lymphoid hyperplasia in the Sca1-HGAL mice

(a) Genes significantly induced or repressed within purified B220+ splenocytes of Sca1-HGAL mice in comparison with wild-type littermates, as determined by SAM using an FDR 10% and demonstrating at least 3-fold change. Each row represents a separate gene and each column a separate mRNA sample from each of 8 mice, with 4 mice from within each group. The level of expression of each gene in each sample, relative to the mean level of expression of that gene across all the samples, is represented using a red–green color scale, extending from fluorescence ratios of 0.25 to 4 (–2 to +2 in log base 2 units). Selected genes are highlighted. (b) Depicted are the relative mRNA expression levels for selected genes exhibiting significant differential expression from (a), including *Igh-2* (IgA), *Ighg1* (IgG1), *Ighg2b* (IgG2b), and *Cd80* (CD80). These genes were independently assessed for differential expression of the corresponding proteins (in parentheses), as depicted in Figure 7a, and panel (c). (c) Induction of CD80 cell surface protein expression in B-cell splenocytes of the Sca1-HGAL mice measured by flow cytometry. Data are representative of 3 mice. (d) Gene set enrichment analysis of the relative representation of differentiation states within

Sca1-HGAL compared to control B-cells. Gene expression data from Sca1-HGAL B-cells showed significant enrichment for signatures corresponding to both Follicular/Marginal Zone and Plasma cell normal murine B-cell differentiation states, suggesting an over-representation of these states within Sca1-HGAL cells. Signatures corresponding to other differentiation states were significantly enriched in control B-cells, suggesting a relative under-representation in Sca1-HGAL B-cells. (e) Detailed view of gene set enrichment analysis results, showing a strong bias of genes from normal Follicular/Marginal zone B-cells (left panel) and Plasma cells (right panel) in Sca1-HGAL B-cells compared to control B-cells.

Author Manuscript

Author Manuscript

Author Manuscript

Author Manuscript